STUDY OF AIRFLOW AROUND SHIP WITH RIGID SAIL ARRAY AND POTENTIAL ARRAY PROPULSIVE POWER

G M Atkinson, Eco Marine Power, Japan and University of Tasmania, Australia

SUMMARY

An array of rigid sails installed on a large powered ship could provide a viable means to reduce fuel oil consumption (FOC) and emissions by using the power of the wind as a source of supplementary propulsion. This paper describes the study of airflow around a concept ship design fitted with 14 segment rigid sails (SRS) using a virtual wind tunnel software application and also investigates the propulsive force that a fixed sail array could provide using computational fluid dynamics (CFD) analysis.

NOMENCLATURE

[Symbol]	[Definition] [(unit)]
3D	three dimensional.
A	area (m^2)
ADV	advection
AoA	angle of attack
AR	aspect ratio
AW	apparent wind
AWA	apparent wind angle
AWS	apparent wind speed (kn or m/s)
C_D	co-efficient of drag
CFD	computational fluid dynamics
CO_2	carbon dioxide
COG	course over ground
C_X	co-efficient of thrust in the direction of ship's movement.
C_X(Max)	maximum co-efficient of thrust in the direction of ship's movement.
DWT	deadweight tonnage/tonnes
EEDI	energy efficiency design index
F_D	drag force
FOC	fuel oil consumption
GRT	gross tonnage/tonnes
HFO	heavy fuel oil
IMO	International Maritime Organization
IPT	Autodesk Inventor part
kn	knot(s)
kW	kilowatt(s)
LOA	length overall
m	metre(s)
MCR	maximum continuous rating
M/E	main engine(s)
M_H	mast height
m/s	metres per second
MW	Megawatt(s)
NT	net tonnage/tonnes
ρ	density of fluid (kg m^{-3})
P	pressure of air (N m^{-2})
Pa	Pascal(s)
PM	particulate matter
PPMAX	post panamax
PV	photovoltaic
rpm	revolutions per minute
RSS	rigid square sail
SD	sail direction

SH	ship's head or ship's heading.
SOG	speed over ground (kn or m/s)
SRS	segment rigid sail
STL	stereolithographic
SST k-ω	shear stress transport k-omega
t	tonne(s)
TED	turbulent energy dissipation
TKE	turbulent kinetic energy
TPD	tonnes per day
υ	Kinematic viscosity (N s m^{-2})
v	velocity (m/s)
vShip	velocity of ship
W	Watt(s)
x, y, z	body axis Cartesian coordinates in the x, y, z-direction

1. INTRODUCTION

In April 2018 the International Maritime Organization (IMO) announced that it had adopted a strategy to reduce greenhouse gas emissions from ships, and this along with other policy initiatives in the shipping industry including the Energy Efficiency Design Index (EEDI), are acting as a catalyst in encouraging the design of ships that are more energy efficient. There is also an increasing focus on the need to reduce the use of heavy fuel oil (HFO) and the resultant airborne emissions including particulate matter (PM) and CO_2. Wind or sail assisted propulsion via the use of rigid sails is one promising technology that could improve the energy efficiency of ships and also lower vessel emissions. On large ships it is likely that multiple sails would be deployed as an array and thus the performance of an array will be an important consideration when incorporating them into future ship designs or retrofitting them to ships already built.

In the current study an array of 14 segment rigid sails (SRS) were arranged in a side by side configuration on a 3D (three dimensional) ship model specifically constructed to incorporate an SRS array. The airflow around the sails and ship was studied and the total drag force (F_D) recorded. The sail array was then isolated from the ship and studied using computational fluid dynamics CFD) based analysis. This enabled the propulsive force in the direction of ships movement to be determined. An

estimate of the total propulsive power a fixed SRS array could provide was also calculated.

2.   RIGID SAIL ARRAY AND ECO SHIP MODEL

2.1   SEGMENT RIGID SAIL (SRS)

A segment rigid sail (SRS) is a type of rigid square sail (RSS) with a curved front and flat rear surface. It is also a very simple aerofoil and the rear surface would typically be facing towards the direction of airflow. This type of rigid sail is capable of providing propulsive power either due to the drag force acting upon it or due to a combination of drag and lift forces. The potential propulsive power that can be provided by a single SRS is related to the forces acting upon it and this in turn is related to the apparent wind speed (AWS) and speed at which the ship is moving (v_{Ship}). This along with other variables such as the total sail area can then be used to create a power profile (Atkinson and Binns, 2018). The power profile and main dimensions for the SRS used in this study are displayed in Table 1.

Table 1. Power profile for SRS with sail area of 100m^2.

Sail Type	Segment Rigid Sail (SRS)		
Ship Speed	12 knots (6.2 m/s)		
Sail Height	12.5m	C_X (Max)	1.4
Chord (Width)	8.0m	Power at 15 m/s	119kW
Aspect Ratio (AR)	1.56	Power at 10 m/s	53kW
Sail Area (A)	100m^2	Power at 5 m/s	13kW

C_X is defined as the maximum co-efficient of propulsive thrust or force and is determined either via wind tunnel testing or via analysis using a CFD software application. For the SRS in this study C_X(Max) was derived from the analysis of the same type of sail in a previous study (Atkinson, 2018). The maximum propulsive power that the sail could provide (P_{MAX}) was calculated using a maximum wind velocity (v) = 15 m/s as it is assumed that at higher wind speeds the sail may be lowered due to safety concerns.

Propulsive power is determined using:

$$P = Fv_{Ship}, \qquad (1)$$

where P is the power (W), F the force (N) and v_{Ship} is the velocity of ship (m/s).

In this paper the velocity of the ship is considered to be equal to the ship's speed over ground (SOG).

The mast height (M_H) was set to 2 m meaning that the bottom surface of the sail would be 2 m above the deck of the ship when the sail was raised. Also for purposes of this study each sail is considered to be capable of being rotated, lowered and raised via a computer control system. However for simplification purpose all sails in the array will be set or rotated to the same position.

2.2   SRS SAIL ARRAY

On a large ocean going ship with sail-assisted propulsion it is envisaged that several sails would be utilized as has been outlined in a number of studies and design concepts. (Fujiwara et al., 2003, Li et al., 2015, Hirayama, 2015, Eco Marine Power, 2012, Burden et al., 2010, Atkinson, 2016). In this study an arrangement of 14 sails has been used as the basis for analysis and designated as an SRS array. This differs from other sail arrangements that locate large sails along or near the centreline of the ship. (Ouchi et al., 2011, Shukla and Ghosh, 2009).

The primary reasons for focusing on the type of SRS array described in this paper are:

- To allow for the sails to be located on either side of the ship as a means to improve stability.
- To allow for the sails to be lowered and stowed.
- To reduce airflow turbulence or interference caused by the sails by limiting the area of each individual sail to 100m² each.

Further details regarding the sail array and its location on the ship are described in the following section.

2.3   ECO SHIP 3D MODEL WITH SRS ARRAY

To study the airflow around a ship fitted with an SRS array several 3D models were created in IPT and STL formats. The design and dimensions of these models were based upon the Aquarius Eco Ship design concept (Eco Marine Power, 2012). This concept was created to illustrate how rigid sails and photovoltaic (PV) panels could be incorporated into the design of a large bulker or cargo ship. The accommodation block and wheelhouse are located near the front of the ship to optimise the shape of the vessel for utilizing an SRS array. The purpose of this arrangement is to minimize the interference these structures would create when the apparent wind (AW) was from astern of the vessel.

14 rigid sails are arranged on the deck of the ship in a side by side configuration with 7 sails in two rows with each row extending down the port and starboard sides.

The distance between each sail would allow for them to be lowered and stored either fore & aft or lowered towards the centreline of the ship. Other methods to lower and store the sails are possible but these are not discussed in this paper. The 3D ship model including overall dimensions and the spacing between the sails is shown in Figure 1.
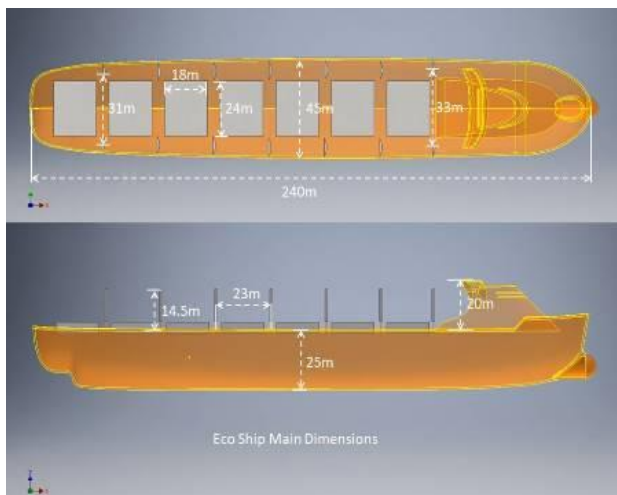

Figure 1. Overview of Eco Ship 3D model with SRS array arranged in side by side configuration.

Table 2. Eco Ship with SRS array main dimensions and specifications.

Eco Ship Main Specifications			
Length (LOA)	240 m	M/E Output @ MCR	15,000 kW @ 90 rpm
Breadth	45 m	M/E Output @ 16 kn	13,000 kW
Gross Tonnage (GRT)	55,500 t	M/E Output @ 12 kn	5,000 kW
Deadweight (DWT)	102,000 t	M/E Output @ 5 kn	1,500 kW
Net Tonnage (NT)	35,000 t	FOC (per day) at design speed	46 t @ 16 kn
Draft	18 m	FOC (per day) at eco speed	22 t @ 12 kn
Design Speed	16 kn	FOC (per day) at low speed	7 t @ 5 kn
Eco Speed	12 kn	Sail Dimensions	12.5 m x 8 m
Low Speed	5 kn	Total Sail Area (14 sails)	1400 m^2

Vessel particulars including installed power, overall length and operating speed (Table 2) are based approximately on the specifications for similar Post Panamax (PPMAX) or large cargo ships currently in service although these are not directly correlated with any one particular ship. Engine power and propulsion trends were also studied to determine the main engine

power ratings most notably "Propulsion trends in bulk carriers" (MAN Diesel & Turbo, 2014).

It should be noted that the ship design and arrangement of sails in this study does not take into account in detail design aspects such as vessel stability, weight of the sails and impact on cargo space. Other limitations as noted in the paper *Considerations regarding the use of rigid sails on modern powered ships* (Atkinson et al., 2018) may also need to be taken into account.

3.   VIRTUAL WIND TUNNEL STUDY

3.1   METHODOLOGY

To observe airflow around the ship model (Figure 1) a virtual wind tunnel software application was used (Autodesk Inc., 2016). The accuracy of this application is stated as being within 6% of those obtained via actual wind tunnel experiments although this accuracy is known to be less at lower air velocities. (Autodesk Inc., 2014). Therefore the primary aim of the simulations was to observe the airflow around the ship and sails and not to determine accurate figures related to drag force and surface pressure.

Models used for simulations were imported into the virtual wind tunnel in STL format at 1/10th scale and the dimensions of the tunnel were initially as per the default settings, but adjusted as the model was rotated around the Z-axis. This was to ensure that the tunnel was set up as per the application guidelines and to confirm there was a sufficient amount of space between the model and the tunnel boundaries. The primary reasons for using a 1/10th scale model were to allow the simulations to stabilize in a reasonable amount of time and to reduce the overall size of the simulation environment. An overview of the orientation of the model inside the virtual wind tunnel is shown in Figure 2.
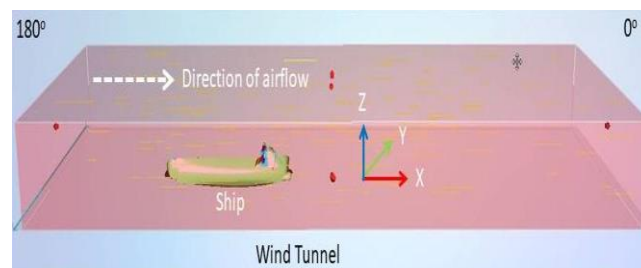

Figure 2. Orientation of ship model inside wind tunnel with rotation around the Z-axis = 0°.

The bottom surface of the wind tunnel was raised slightly so that the lower part of the hull was not exposed to airflow. This was to simulate the ship sitting in the water and thus airflow under the hull would not be possible.

Simulations were conducted with the array being set at sail direction (SD) 0° and 345°. SD represents the

direction the front surface of the sail is facing relative to the base of the mast and is expressed as an angle between 0º and 360º (Figure 3). It can also be expressed as an angle between 0º and 180º port or starboard and this might be useful in communicating the position of the sails to the crew or for remote monitoring purposes.

The air velocity for all simulations was set at the inlet to 5 m/s (or approximately 9.7) knots and the simulation resolution set to 150. The air velocity of 5 m/s represents a gentle breeze according to the Beaufort wind force scale (UK Met Office) and would often be encountered by an ocean-going ship according to the Global Wind Probability Matrix (International Maritime Organization (IMO), 2011).
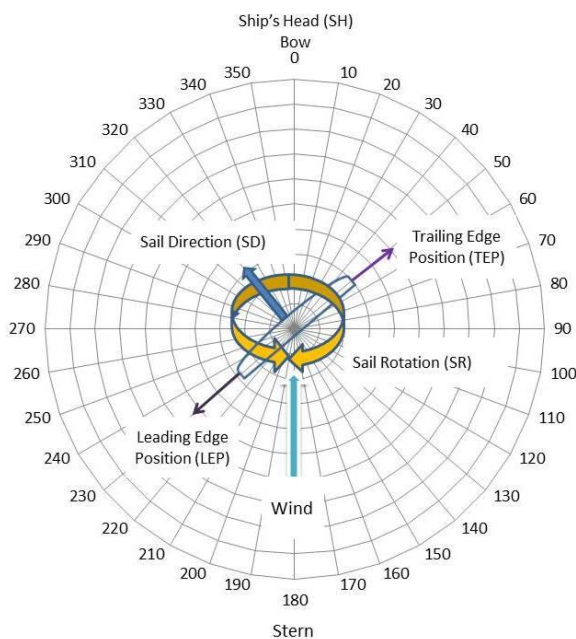

Figure 3. Overview of SRS position indicators.

3.2 SHIP WITH SRS ARRAY AT SAIL DIRECTION 0º.

The first simulation was conducted with the ship orientated as shown in Figures 2 & 4. The wind tunnel for this simulation was 114 m in length (l), 22 m wide (w) and 13 m high (h). Additional simulations were then conducted as the ship was rotated in 15º steps about the Z-axis and the dimensions of the wind tunnel were adjusted as required. As the ship model was rotated around the Z-axis this effectively altered the ship's heading (SH) and the angle between the rear surface of the sail and the direction of airflow. This angle is designated as the angle of attack (AoA).

The leading edge position (LEP) and trailing edge position (TEP) of a sail at SD 320º are shown in Figure 3. As with SD, the LEP and TEP could also be expressed as 0º -180º port or starboard. When the apparent wind angle is perpendicular to the rear surface of the sail the

AoA will equal 90º and in that case the port edge of the sail is designated the LEP. In addition to providing a reference point, the LEP could also be utilized by a computer automation system to rotate the sail to the desired SD based on the AWA without any manual input or action by the crew.

For each simulation the airflow and surface pressures were observed and the total drag force and average drag co-efficient (C_D) for each ship heading are displayed in Table 3.

Table 3. Drag co-efficient & drag force at selected headings for Eco Ship with SRS array at SD = 0º and air velocity of 5 m/s.

Eco Ship with SRS array at Sail Direction 0º				
SH	**AWA**	**AoA**	**C_D**	**Drag**
0º	180º	90º	0.69	179N
345º	165º	75º	0.54	258N
330º	150º	60	0.60	428N
315º	135º	45º	0.78	705N
300º	120º	30º	0.79	782N
285º	105º	15º	0.84	867N
270º	90º	0º	0.96	958N

When the airflow was from directly astern two long elongated tubular columns of lower velocity airflow were present around each row of sails and this could be visualized using an iso-surface plot with the plot air velocity set to 2 m/s (Figure 4). Areas of high pressure were also observed on the rear surfaces of the 2 sails near the stern, on the rear of the accommodation block, and the on the surface of the hull near the stern. These areas were highlighted by orange and red shading and are shown in the lower image in Figure 4. These 4 surface areas together were responsible for most of the drag when the airflow was from directly astern and thus it could be feasible to modify the shape or profile of these areas to further increase drag. This type of modification could potentially lead to an increase in propulsive force resulting from winds coming from this direction.

As the ship model was rotated the airflow turbulence caused by the sails gradually decreased and drag caused by the hull and superstructure increased. This could be determined by observing the pressure contours on the surfaces of the sails, hull and superstructure. It was also observed that as the AWA moved towards the beam the airflow was noticeably deflected over the deck as it moved against the hull. This deflection could result in less air moving onto and around the sail surfaces if the sails were located close to the sides of the ship and/or mounted on low masts close to the deck.

When the ship was rotated to a heading of 270º this resulted in the AW coming from directly abeam. Air moved freely between the sails with only the leading edges of the port side row of sails displaying regions of

surface pressures in excess of 5 Pa or 5 N/m². In this position the sails were effectively feathered and the AoA = 0°. In this orientation the major sources of aerodynamic drag were the superstructure and hull. Vectors of airflow across the ship and between the sails for this simulation are shown in Figure 5 along with the surface pressure contours. With the ship model at this orientation the virtual wind tunnel dimensions were 110 m (l) x 59 m (w) x 12 m (h).
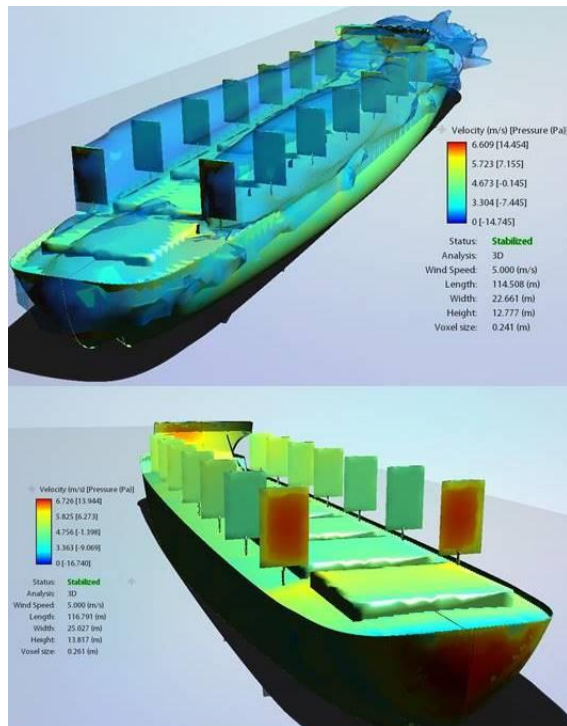

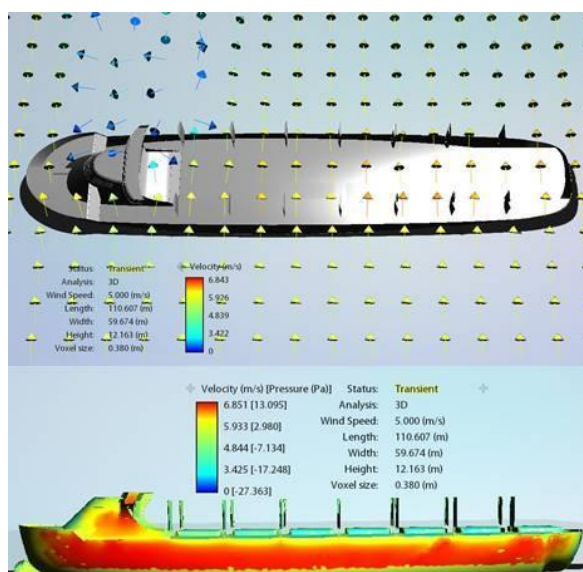Figure 4. Eco Ship model with SRS array at SD 0°, AWA 180° & AoA 90°.

Figure 5. Airflow vectors and surface pressure contours for Eco Ship model with SRS array at SD 0° & AWA 90°.

3.3 SHIP WITH SRS ARRAY AT SAIL DIRECTION 325°.

Since it has been previously determined that a rigid sail of the type used in this study will potentially provide the maximum propulsive power at an AoA of approximately 35° (Atkinson, 2018), the next series of simulations were conducted with SD = 325° or SD 35° port. As with the previous series of simulations the ship model was rotated around the Z-axis in 15° steps so that airflow was towards the rear surfaces of the sails. The first simulation was conducted with the ship orientated as per Figure 2 and the dimensions of the virtual wind tunnel were approximately the same as those for the ship with the sail array at SD 0°.

As with the simulations discussed in section 3.2 total drag force and the average drag co-efficient (C_D) were recorded and are listed in Table 4.

Table 4. Drag co-efficient & drag force at selected headings for Eco Ship with SRS array at SD = 325° and air velocity of 5 m/s.

Eco Ship with SRS array at Sail Direction 325°				
SH	AWA	Array AoA	C_D (Avg)	Drag Force
0°	180°	55°	0.61	162N
15°	165°	70°	0.51	244N
30°	150°	85°	0.58	415N
45°	135°	90°	0.68	640N
60°	120°	65°	0.72	719N
75°	105°	50°	0.86	974N
90°	90°	35°	0.93	978N

As observed when the array SD was 0° the airflow around the rows of sails created tubular areas of lower air velocity but the area of these regions appeared smaller in size. As the model was rotated in 15° steps the surface pressure on the sails increased to maximum when the AWA = 135° and the AoA = 90° at which point drag created by the sails and ship was 640 N.

When the ship model was rotated to a heading of 090° the AoA for the sails = 35° (Figure 6). At this point each sail would be close to operating at its maximum thrust co-efficient C_X(Max) although the airflow onto the downwind row of sails was decreased due to the interference caused by the upwind row of sails. This could be observed by the decreased surfaces pressures on the sails on the downwind side especially along the leading edges.
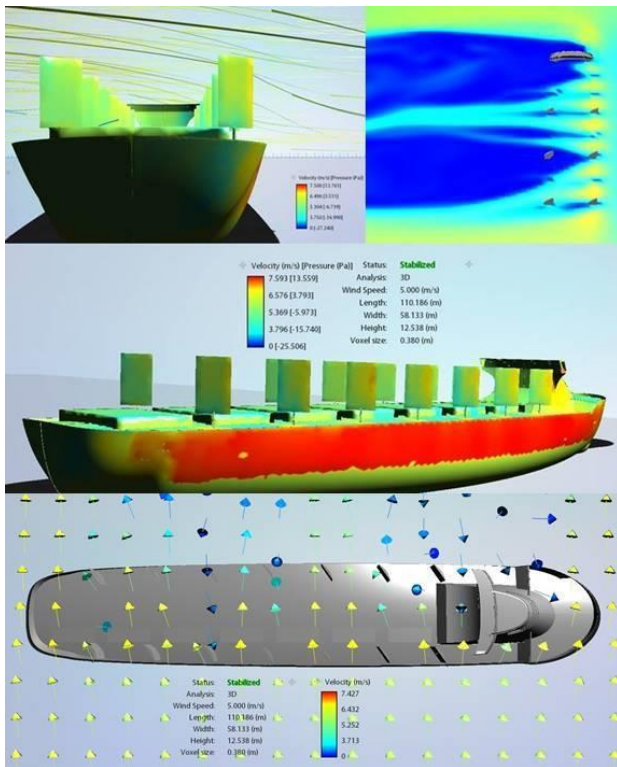
Figure 6. Eco Ship model with SRS at SD direction 325º, AWA 90º and AoA 35º.

With the ship at this orientation the wind tunnel dimensions were 112 m (l) x 67 m wide x 14 m (h).

3.4 ANALYSIS AND DISCUSSION

The observation of airflow and surface pressures using the 3D Eco Ship model indicated that estimating the propulsive forces from a sail array by multiplying the potential propulsive power of each sail by the total number of sails would provide inaccurate results. This is due to the air velocity moving onto and around the sails being affected by other sails in the array. As a result the propulsive force that could be provided by each sail may vary considerably.

The minimum drag force observed was 162 N and this occurred when the SRS array was at SD 325º and the AWA was 180º. This compared to 179 N when the ship was at the same orientation with the array SD at 5º and illustrated how the drag of the array was reduced by lowering the AoA for each sail. However due to the imprecise nature of the drag measurements this cannot be stated for certain and this topic needs to be studied further.

The maximum drag observed was when the full side profile of the ship was directly perpendicular to the flow of air and there was little difference in the total drag force when the sail array was set at SD 0º or SD 325º with the drag being 958 N and 978 N respectively. This suggests that with the sail array at either of those

positions that it is not a significant source of drag or side force. This however is a topic that requires further investigation. The highest surface pressures observed were in the range of approximately 13.5 – 15Pa and not surprisingly were when the ship and sail surfaces were perpendicular to the airflow.

It needs to be remembered though that the model used for these simulations was $1/10^{th}$ scale therefore to approximate the drag forces for a full scale vessel the results should be multiplied by a factor of 10.

4. CFD ANALYSIS OF RIGID SAIL ARRAY

4.1 METHODOLOGY

Although the simulations using the virtual wind tunnel were useful for observing airflow, surface pressures and total drag, this information alone was not sufficient to allow for estimates to be made regarding the total propulsive power a sail array could provide. To obtain the additional data to needed for these estimates another set of simulations were conducted using a CFD application (Autodesk Inc, 2018) using the same SRS array layout as used for the Eco Ship simulations. This array is shown in Figure 7.
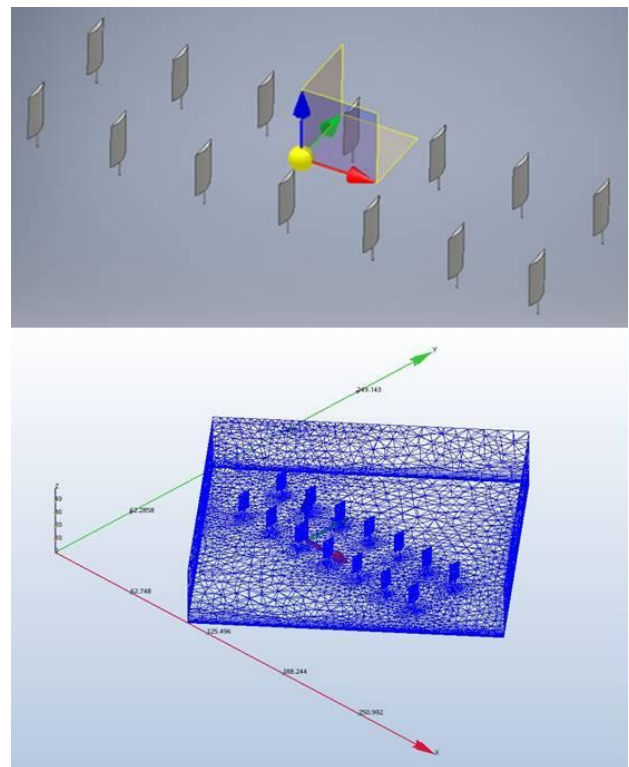

Figure 7. SRS sail array at SD 0º and AWA 150º.

For the CFD simulations the SRS model was created in IPT format and imported in the CFD simulation environment at full scale meaning that each 3D sail was 12.5 m (h) x 8.0 m (w) (Table 1). Consequently the size

of the volume created around the sail array was very large with the total simulation area being approximately 2 million square metres (m²) in some cases. Thus the meshing of the volume needed to be carefully managed otherwise the total number of elements could become very large. In cases where this happened it not only caused the time to reach convergence to increase considerably but also often resulted in the simulation failing to reach convergence.

An example of the orientation of the sail array in relation to the volume of air surrounding it is shown in Figure 7. The X-axis is indicated by the red arrow, the Y-axis by the green arrow and the Z-axis using a blue arrow. In this example the volume of air around the sail array has been offset along the Z-axis by 30° by to simulate an AWA of 150°. This in turn results in the AoA for each sail in the array being 60°. For most simulations SD = 0° although one series of simulation were conducted with the SD at 330° and this will be discussed later.

The SRS array remained aligned with the X-axis and thus force along this axis represented the propulsive force that the sail array would produce in the direction of ships movement under normal operating conditions. The mesh and solution settings were derived from those used for the analysis of a stand-alone segment rigid sail (Atkinson, 2018). These setting are summarised in Table 5.

Table 5. Summary of mesh settings for SRS array CFD simulations.

Turbulence Model	SST K-Omega
Advection Scheme	ADV 1
Layers	15
Later Gradation	1.25
Layer Factor	0.84
Solution Control	Auto. Tight convergence.

The turbulence model used was SST K-Omega (SST k-ω). This is a two-equation eddy-viscosity model incorporating turbulent kinetic energy (TKE) and turbulent energy dissipation (TED) equations (Autodesk Inc., 2017). For advection (ADV) the default scheme was used: ADV 1.

The dimensions of the volume of air surrounding the SRS model varied from approximately 260 m (l) x 140 m (w) x 40 m (h) when Z-axis rotation = 0° to 140 (l) x 220 (w) x 40 m (h) when Z-axis rotation = 90°.

4.2.   RESULTS AND ANALYSIS

The main series of simulations comprised of 10 test cases starting with the AWA = 180°. For each subsequent test case the volume of air around the sail array was rotated or offset in 10° increments until the airflow was from the side of the SRS array or AWA = 90°. For these simulations the sails were fixed at SD 0° and thereby the

front curved surface of each sail would face towards the bow of the ship and the rear surface towards the stern. Although it might be desirable to alter the AoA for the SRS array as the AWA changed (as noted in the previous section) this was not done for the main CFD simulations as the study is focused on a simple implementation of a sail array, meaning that the sails were fixed and not rotatable.

For all simulations or test cases in the section the total force along the X-axis (F_X) and the calculated co-efficient of thrust (C_X) are listed in Table 6.

C_X was calculated using:

$$C_X = \frac{F_X}{0.5\ \rho v^2 A} \qquad (2)$$

where C_X is the thrust coefficient, ρ of the fluid (1.2 kg/m³ for air at sea level at 20°C), v is the flow velocity (m/s) and A is the lift characteristic area of the body (m²).

Table 6. Total force and thrust co-efficient for SRS array at SD = 0° and air velocity of 5 m/s.

SRS Array at SD = 0°				
Z-Axis	AoA	AWA	F_X	C_X
0	90	180	13504 N	0.64
10	80	170	19560	0.93
20	70	160	23015	1.10
30	60	150	25995	1.24
40	50	140	24854	1.18
50	40	130	23444	1.12
60	30	120	25111	1.20
70	20	110	19507	0.93
80	10	100	11190	0.53
90	0	090	3144	0.15

As observed during the virtual wind tunnel simulations when the AWA = 180° and the SD = 0° (Figure 4) only the two rear sails were directly in the path of the airflow. The drag force created by the SRS array though was greater than the force acting on the rear two sails alone. For example a single SRS with similar dimensions subjected to an airflow of 5.1 m/s & set at an AoA = 90° was found to produce a drag force of approximately 2275 N (Atkinson and Binns, 2018) and thus for two sails a theoretical estimate of 4550 N could be derived. However as can be seen from Table 4 this is less than half of the drag force recorded during the CFD simulation at AWA = 180°. This was most likely due to the regions of reduced airflow around each row of sails creating additional pressure drag and this is similar to the drag created by vehicles travelling in close proximity (Browand, 2005). It is therefore important to note again that the performance of a sail array cannot simply be determined by calculations based on results from a single

and isolated sail. For this simulation the array Cx was calculated to be 0.64 and due to the alignment of the SRS array this was also the value for C_D. This represents a lower drag co-efficient than the 1.34 calculated for a single isolated SRS (Atkinson, 2018).

As the AW direction moved towards the side of the array F_X increased until AoA = 60° after which F_X varied within a fairly narrow range until declining when the SRS array AoA moved past 30°. This implied that although the SRS array remained in a fixed position that it was still able to provide a relatively stable source of supplementary propulsive power even as the AWA varied if the air velocity remained constant.

As the AWA moved toward the beam the flow of air between the sails became less disturbed and an example of this is shown in Figure 8.
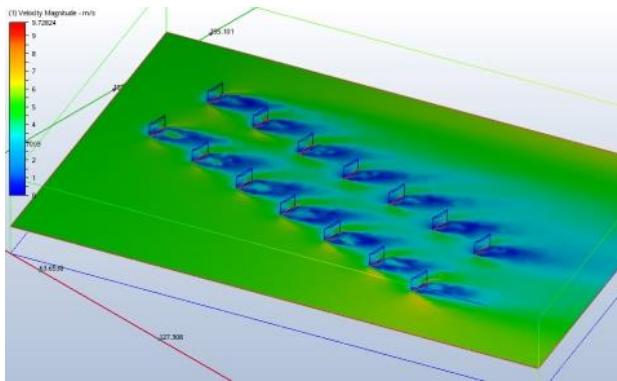

Figure 8. Velocity contours around section of SRS array at SD 0° and AWA 160°.

The presence of wakes behind each sail (Figure 8) was observed by placing a plane to view air velocity contours aligned with the Z-axis. This revealed that air was flowing relatively unimpeded onto and around all sails in the array. The propulsive force resulting from the sails for this test case was 23015 N.

When the airflow was directly from the side of the array the AoA = 0° and the force exerted by the array along the X-Axis was only 3144 N due to the small amount of lift being created as airflow moved over the curved surfaces of the sails. Also for this particular test case drag force equalled side force and a total of 1466 N was observed along the Y-Axis.

The maximum force observed during along the X-Axis for all test cases was 25995 N. This occurred when the volume around the SRS array was set to represent an AWA of 150° and at this point C_X = 1.24.

A supplementary test case was also performed to investigate if the sail array direction could be altered to increase propulsive force. In this simulation the AWA was 90° and each sail in the array was rotated and set at SD 330° (Figure 9).
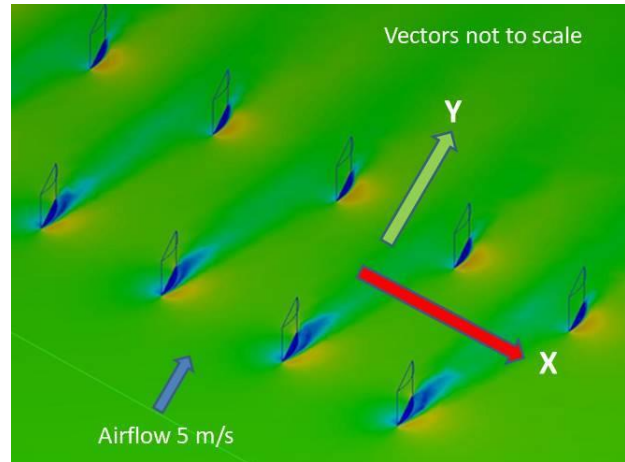

Figure 9. Velocity contours around section of SRS array at SD 330° and AWA 90°.

In this test case the total propulsive force observed was 21713 N and this was 150% greater when compared to the 3144 N when the sail array was set at SD = 0° (Table 6). It can therefore be concluded that the propulsive power provided by an SRS array can be optimized by adjusting the positions of the sails. Additionally it might be possible to further optimize the performance of the sail array by adjusting the positions of the sails individually as opposed to moving all sails to the same position.

Lastly as an indication of how much propulsive power an SRS array could provide the array P_{MAX} was calculated using Formula 1 based on the maximum value of F_X from Table 6 and a ship velocity of 6.2 m/s. Using these figures PMAX was determined to be 156 kW. It should be noted however that this figure is for an SRS array with all sails at SD = 0° and not optimised to best suit the AWA.

7. CONCLUSIONS

A relatively simple rigid sail array could be an effective means to reduce fuel oil consumption on ships by acting as a supplementary source of emissions-free propulsion. In this study the airflow around an array of 14 segment rigid sails on an Eco Ship and the performance of the sail array itself was investigated.

Key findings and conclusions resulting from this study are listed below:

- A bulk carrier or similar ship with the wheelhouse and accommodation block located towards the bow could be well suited to utilize an SRS array as a source of supplementary propulsion.
- Estimating the propulsive force that could be potentially provided by a rigid sail array should not be calculated using only the performance characteristics of a single stand-alone sail.

- A SRS array with 14 sails arranged in a side by side configuration could potentially provide 25111 N of propulsive force at an AWS of 5 m/s.
- The propulsive force provided by the sail array could be increased significantly by adjusting the position of the sails as the apparent wind direction changes.
- It may be possible to further optimise the performance of the sail array by positions the sails individually rather than moving all sails in the array to the same positions.
- The design and dimensions of the Eco Ship may need to be adjusted to take into account such issues as the vessels stability, the amount of space available to carry cargo and the optimum arrangement of the sails.
- A variation of the Eco Ship with the wheelhouse and accommodation block towards the front of the vessel should be studied to determine the impact of this arrangement on the performance of the SRS array.

Furthermore a number of areas require further research including; the performance analysis of differing rigid sail arrangements, the automated control of rigid sail arrays and optimizing ship designs for the use of rigid sails and other wind-assisted propulsion devices.

8. REFERENCES

The Eco Ship drawings and 3D model contained in this paper were based on and derived from the Aquarius Eco Ship design concept developed by Eco Marine Power. Co. Ltd. (Japan).

9. REFERENCES

1. ATKINSON, G., BINNS, J. & NGUYEN, H. 2018. *Considerations Regarding the Use of Rigid Sails on Powered Ships*. Cogent Engineering, 5**,** 20.
2. ATKINSON, G. M. 2016. *Power module for use in marine vessel, and wind-propelled vessel provided with said power module*. United States patent application.
3. ATKINSON, G. M. 2018. *Analysis of lift, drag and CX polar graph for a 3D segment rigid sail using CFD analysis*. Journal of Marine Engineering & Technology**,** 1-11.
4. ATKINSON, G. M. & BINNS, J. 2018. *Power Profile for Segment Rigid Sail*. Journal of Marine Engineering & Technology, 17**,** 99-105.
5. Autodesk Inc. 2018. *Computational fluid dynamics software* [Online]. Author. Available: https://www.autodesk.com/products/cfd/overview [Accessed 2018].
6. Autodesk Inc. 2014. Flow Design Validation Study: Automotive Drag. Author.
7. Autodesk Inc. 2016. *Flow Design | Virtual Wind Tesing Software* [Online]. Author. Available: http://www.autodesk.com/products/flow-design/overview [Accessed 2016].
8. Autodesk Inc. 2017. *SST K-Omega Turbulence Models* [Online]. Author. Available: https://knowledge.autodesk.com/support/cfd/learn-explore/caas/CloudHelp/cloudhelp/2016/ENU/SimCFD-Learning/files/GUID-0F5C4828-9F91-46B6-A16A-2578D72DCFCC-htm.html [Accessed 2017].
9. BROWAND, F. 2005. *Reducing Aerodynamic Drag and Fuel Consumption*. Global Climate and Energy Project Workshop on Advanced Transportation. Stanford University.
10. BURDEN, A., LLOYD, T., MOCKLER, S., MORTOLA, L., SHIN, I. B. & SMITH, B. 2010. *Concept design of a fast sail assisted feeder container ship*.
11. Eco Marine Power. 2012. *Aquarius Eco Ship* [Online]. Eco Marine Power Co., Ltd. Available: http://www.ecomarinepower.com/en/aquarius-eco-ship [Accessed 2016].
12. FUJIWARA, T., HIRATA, K., UENO, M. & NIMURA, T. *On Development of High Performance Sails for an Ocean Going Sailing Ship*. International Conference on Marine Simulation and Ship Manoeuvrability (MARSIM '03), 2003 Kanazawa. National Maritime Research Institute (Japan).
13. HIRAYAMA, A. 2015. *Research and Development into Practical Applications of Power Assist Sails*. Tokyo: ClassNK.
14. International Maritime Organization (IMO) 2011. *Global Wind Specification along the Main Global Shipping Routes to be applied in the EEDI Calculation of Wind Propulsion Systems*. MEPC 62/INF.34.
15. LI, Q., NIHEI, Y., NAKASHIMA, T. & IKEDA, Y. 2015. *A study on the performance of cascade hard sails and sail-equipped vessels* Ocean Engineering, 98**,** 23–31.
16. MAN Diesel & Turbo 2014. *Propulsion trends in bulk carriers*. Copenhagen SV, Denmark: MAN Diesel & Turbo,.
17. OUCHI, K., UZAWA, K. & KANAI, A. *Huge Hard Wing Sails for the Propulsor of Next Generation Sailing Vessel*. Second International Symposium on Marine Propulsors, 2011 Hamburg.
18. SHUKLA, P. C. & GHOSH, K. 2009. *Revival of the Modern Wing Sails for the Propulsion of Commercial Ships*. International Journal of Environmental Science and Engineering, 1.
19. UK Met Office. *Beaufort wind force scale* [Online]. Author. Available: http://www.metoffice.gov.uk/guide/weather/marine/beaufort-scale [Accessed 2016].